

Parallel Newton methods for the continuous quadratic knapsack problem: A Jacobi and Gauss-Seidel tale

L. D. Secchin ^{*} P. J. S. Silva [†]

March 18, 2026

Abstract

The continuous quadratic knapsack (CQK) problem involves minimizing a diagonal convex quadratic function subject to box constraints and a single linear equality constraint. It has numerous applications in resource allocation, multicommodity flow, machine learning, and classical optimization tasks such as Lagrangian relaxation and quasi-Newton updates. In this work, we revisit the semismooth Newton method introduced by Cominetti, Mascarenhas, and Silva. We demonstrate that the method can be significantly improved in two directions. First, for projections onto the simplex or the ℓ_1 -ball, it can incorporate Condat's highly effective initial multiplier guess. Second, it can serve as a flexible foundation for CQK algorithms, allowing for different parallel variants tailored to exploit CPU and GPU computational models. These improvements are implemented in the open-source Julia package `NewtonCQK.jl`. We present extensive numerical tests comparing this implementation with other state-of-the-art solvers, demonstrating its superior efficiency and scalability.

1 Introduction

The nonlinear knapsack problem is a classical model in operations research and finance; see [28, 7, 1, 9, 29, 30] and references therein. In its most general form, it can be stated as

$$\min_x f(x) \quad \text{s.t.} \quad g(x) \leq b, \quad x \in S,$$

where $f, g : \mathbb{R}^n \mapsto \mathbb{R}$, b is a real constant, and S is a nonempty closed set. That is, it is a nonlinear optimization problem with a single inequality constraint and abstract constraints. When the functions are separable and the abstract constraint S represents a box, the model is also known as the continuous nonlinear resource allocation problem [29]. Such models find applications in hierarchical planning systems [7], portfolio selection, resource allocation [10, 8], video on-demand services [29], batching [29], capacity and production planning [9], multicommodity flows [32], and support vector machines [17, 21, 14], among many others.

In this paper, we consider the particular case known as the *Continuous Quadratic Knapsack problem* (CQK) [17, 14], defined as

$$\min_x \frac{1}{2} x^t D x - a^t x \quad \text{s.t.} \quad b^t x = r, \quad l \leq x \leq u, \quad (\text{CQK})$$

where $x \in \mathbb{R}^n$, $D = \text{diag}(d_1, \dots, d_n)$ is a positive diagonal matrix, $l \leq u$ are the lower and upper vector bounds on x , respectively. Some bounds may be $\pm\infty$. We assume throughout the text that $b > 0$. This condition can be satisfied by eliminating variables or reverting their sign where necessary. Since D is positive definite, (CQK) is equivalent to the Euclidean projection of $D^{-1}a$ onto the feasible region. It encompasses the problem of projecting a point y onto the r -simplex:

$$\min \frac{1}{2} \|x - y\|^2 \quad \text{s.t.} \quad x \in \Delta = \left\{ x \in \mathbb{R}^n \mid \sum_{i=1}^n x_i = r, \quad x \geq 0 \right\}. \quad (\text{proj}_\Delta)$$

^{*}Department of Applied Mathematics, Federal University of Esp rito Santo, ES, Brazil. Email: leonardo.secchin@ufes.br

[†]Department of Applied Mathematics, Universidade Estadual de Campinas, Campinas, SP, Brazil. Email: pjssilva@ime.unicamp.br

Indeed, (proj_Δ) is, up to a constant in the objective function, the special case of (CQK) with $D = I$, $a = y$, $b_i = 1$, $l_i = 0$, and $u_i = \infty$ for all i . Furthermore, this problem is intrinsically linked to the projection of y onto an ℓ_1 -ball of radius r

$$\mathcal{B} = \left\{ x \in \mathbb{R}^n \mid \sum_{i=1}^n |x_i| \leq r \right\},$$

which can be reduced to the projection of the vector of absolute values of y onto the unit simplex, subsequently restoring the original signs [19]. Note that (CQK) and its variants appear naturally when solving a continuous version of the general knapsack problem using methods based on projected gradient methods, when the functional constraint is linear. They also appear in the subproblems of algorithms that linearize a nonlinear constraint, such as sequential quadratic programming [27]. In turn, the continuous knapsack problems appear as relaxations used in branch-and-bound methods needed when integrality is required [9].

Many methods to solve (CQK) , and especially to project onto Δ or \mathcal{B} , have emerged in the literature. The most prominent ones employ variable-fixing techniques, originally proposed by Michelot in [26]. In particular, to the best of our knowledge, Condat’s variable-fixing algorithm is the fastest (sequential) algorithm for projecting onto Δ [15].

Later, Dai and Chen introduced a general framework to parallelize variable-fixing methods [16]. They proved that if a variable is fixed at a bound within a subproblem, formed by a subset of the coordinates, it remains fixed at the same bound in the original problem. This property allows for the estimation of most of the fixed variables by splitting the full problem into smaller subproblems that are solved in parallel. After this initial phase, the original problem is solved in a reduced form with a significant portion of its variables already fixed. This technique was used successfully to parallelize Condat’s method, resulting in a very efficient implementation.

Another approach, introduced in [14], exploits the fact that (CQK) is a strictly convex problem with simple bounds. Hence, it can be solved through its dual. The authors proposed a globally convergent semismooth Newton method to solve the dual problem, leveraging its simple structure. The method is also very efficient and can be combined with variable-fixing strategies.

In this paper, we present improvements to the semismooth Newton method with optional variable fixing. First, we show that it is possible to adapt the Gauss-Seidel strategy used by Condat, thereby improving performance. We also demonstrate that the resulting method is directly parallelizable without using Dai and Chen’s approach. This is possible because our algorithm employs the dual function to drive convergence instead of relying on variable-fixing for that purpose. However, while the indirection required to implement variable-fixing works well on CPUs, it is not well suited for GPU implementations. This suggests an alternative GPU variation of the algorithm that entirely removes variable-fixing, resulting in a method with a fully decoupled iteration, similar to the Jacobi method for linear systems.

Such developments lead to a new high-performance Julia implementation that is openly available. It includes sequential, parallel, and GPU implementations of the semismooth Newton method, together with specialized variants to project onto Δ and \mathcal{B} . The sequential algorithm for (proj_Δ) generally outperforms even the original C implementation of Condat’s method. Furthermore, the parallel Newton code outperforms the parallel version of Condat’s algorithm by Dai and Chen. Finally, the GPU implementation is shown to be highly effective for large-scale problems.

The paper is organized as follows. In Sections 2.1 and 3, we recall the sequential Newton method for (CQK) and important particular cases, notably for (proj_Δ) . In Section 4, we explain how it can be parallelized. Section 5 is devoted to numerical tests, showing that our proposal outperforms state-of-the-art methods in the literature. Finally, Section 6 presents our conclusions and outlines directions for future work.

Notation $P_C(z)$ denotes the Euclidean projection of z onto a given convex set C . $|I|$ denotes the cardinality of a finite set I . We define $\text{sgn}(t)$ as 1 if $t > 0$, -1 if $t < 0$, and 0 if $t = 0$.

2 Sequential methods for CQK

In this section, we review the two primary frameworks for solving (CQK). The first is based on Newtonian methods. A secant variation was introduced in [17], which was later extended into a fully semismooth Newton method by Cominetti, Mascarenhas, and Silva [14]. Our presentation is based on the latter. The second approach relies on variable fixing techniques, see [26, 22, 23, 15]. We focus on Condat’s variant [15], which incorporates a Gauss-Seidel acceleration that is highly effective in practice.

2.1 Newton methods for CQK

Dualizing only the linear constraint $b^t x = r$ in (CQK), we obtain the dual problem

$$\max_{\lambda \in \mathbb{R}} F(\lambda), \quad F(\lambda) := \min_{l \leq x \leq u} \frac{1}{2} x^t D x - a^t x + \lambda(r - b^t x).$$

One can then easily show that the vector $x(\lambda) \in \mathbb{R}^n$ that attains the minimum in the definition of the dual objective is given by,

$$\forall i = 1, \dots, n, \quad x(\lambda)_i = P_{[l_i, u_i]}((b_i \lambda + a_i)/d_i) = \max\{l_i, \min\{u_i, (b_i \lambda + a_i)/d_i\}\}. \quad (1)$$

Using basic duality results, primal-dual optimality is achieved when this vector is primal feasible. That is, the condition

$$\varphi(\lambda) = r, \quad \varphi(\lambda) := b^t x(\lambda) = \sum_{i=1}^n b_i \max\{l_i, \min\{u_i, (b_i \lambda + a_i)/d_i\}\} \quad (2)$$

is equivalent to the optimality of λ for the dual problem and $x(\lambda)$ for (CQK). Therefore, (CQK) is equivalent to solving the nonlinear equation

$$\varphi(\lambda) = r.$$

The main idea in [14] is to apply a (semismooth) Newtonian strategy to this equation. Since the functions $\lambda \rightarrow P_{[l_i, u_i]}((b_i \lambda + a_i)/d_i)$ are piecewise linear, so is φ and its graph possibly changes the slope exactly at the *breakpoints*

$$\underline{l}_i = (d_i l_i - a_i)/b_i \quad \text{and} \quad \bar{u}_i = (d_i u_i - a_i)/b_i.$$

Also, observe that the lateral derivatives of φ are non-negative and given by

$$\varphi'_+(\lambda) = \sum_{i \mid \underline{l}_i \leq \lambda < \bar{u}_i} b_i^2/d_i \quad \text{and} \quad \varphi'_-(\lambda) = \sum_{i \mid \underline{l}_i < \lambda \leq \bar{u}_i} b_i^2/d_i, \quad (3)$$

see Figure 1(a). The function φ is non-decreasing and may be constant between consecutive breakpoints as depicted in Figure 1(b). Consequently, given λ_k , the Newtonian step depends on whether $\varphi(\lambda_k) < r$ or $\varphi(\lambda_k) > r$. In the first case, λ must be increased. Thus $\varphi'_+(\lambda_k)$ is used, if not zero. Otherwise, λ_k must be decreased, and $\varphi'_-(\lambda_k)$ is employed. If the appropriate lateral derivative is zero, the closest breakpoint in the required direction is computed instead. The complete method is presented in Algorithm 1. Note that it also incorporates a secant update to avoid poor Newton steps, an idea inspired by the pure secant method suggested in [20].

The secant step (line 18) is used to avoid cycling [14]. It computes the zero of the affine function whose graph interpolates $(\underline{\lambda}, \varphi(\underline{\lambda}))$ and $(\bar{\lambda}, \varphi(\bar{\lambda}))$, where the interval $[\underline{\lambda}, \bar{\lambda}]$ contains the optimal λ^* , hence the name “secant”. Necessarily, the resulting λ_S belongs to $(\underline{\lambda}, \bar{\lambda})$. This approach is slightly simpler than the secant step in [14, Algorithm 2]. Here, we leave the analysis of whether $\lambda_{k+1} = \lambda_S$ lies on a non-optimal plateau to the next iteration. Thus, the value $\varphi(\lambda_{k+1}) = \varphi(\lambda_S)$ is computed at the next iteration and the method proceeds normally. This strategy is sufficient for the global convergence of Algorithm 1 according to [14, Theorem 1].

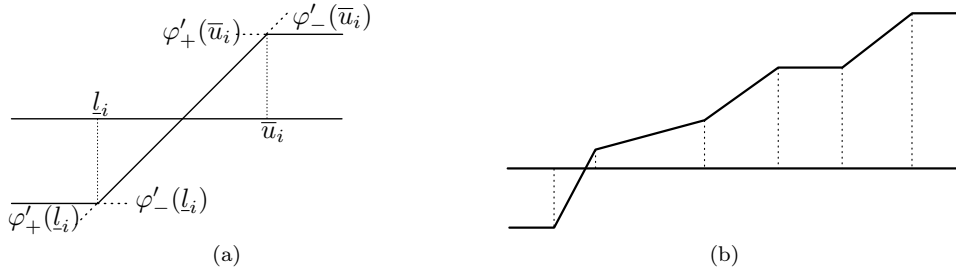


Figure 1: (a) Lateral slopes of $\max\{l_i, \min\{u_i, (b_i\lambda + a_i)/d_i\}\}$ at breakpoints. (b) A typical plot of $\varphi(\cdot) - r$.

Algorithm 1 Semi-smooth Newton method for solving (CQK)

Require: the initial dual estimate λ_0

- 1: Set $k \leftarrow 0$, $\underline{\lambda} \leftarrow -\infty$ and $\bar{\lambda} \leftarrow \infty$
 - 2: **if** $\varphi(\lambda_k) = r$ **then**
 - 3: Stop and return $x(\lambda_k)$ as the solution of (CQK)
 - 4: **if** $\varphi(\lambda_k) < r$ **then**
 - 5: Update $\underline{\lambda} \leftarrow \lambda_k$
 - 6: **if** $\varphi'_+(\lambda_k) > 0$ **then**
 - 7: Define $\tilde{\lambda}_k = \lambda_k - \frac{\varphi(\lambda_k) - r}{\varphi'_+(\lambda_k)}$
 - 8: **If** $\tilde{\lambda}_k < \bar{\lambda}$, define $\lambda_{k+1} = \tilde{\lambda}_k$ and go to line 19. **Otherwise**, go to line 18
 - 9: **else**
 - 10: Define λ_{k+1} as the closest breakpoint to the right of $\underline{\lambda}$ and go to line 19. **If no such breakpoint exists**, stop declaring (CQK) infeasible
 - 11: **if** $\varphi(\lambda_k) > r$ **then**
 - 12: Update $\bar{\lambda} \leftarrow \lambda_k$
 - 13: **if** $\varphi'_-(\lambda_k) > 0$ **then**
 - 14: Define $\tilde{\lambda}_k = \lambda_k - \frac{\varphi(\lambda_k) - r}{\varphi'_-(\lambda_k)}$
 - 15: **If** $\tilde{\lambda}_k > \underline{\lambda}$, define $\lambda_{k+1} = \tilde{\lambda}_k$ and go to line 19. **Otherwise**, go to line 18
 - 16: **else**
 - 17: Define λ_{k+1} as the closest breakpoint to the left of $\bar{\lambda}$ and go to line 19. **If no such breakpoint exists**, stop declaring (CQK) infeasible
 - 18: Define λ_{k+1} as the secant step in $[\underline{\lambda}, \bar{\lambda}]$
 - 19: Set $k \leftarrow k + 1$ and go to line 2
-

As suggested in [14], the initial dual variable λ_0 can be defined as

$$\lambda_0 = \frac{r - s}{q}, \quad s = \sum_{i \in J} \frac{b_i a_i}{d_i}, \quad q = \sum_{i \in J} \frac{b_i^2}{d_i}, \quad (4)$$

with $J = \{1, 2, \dots, n\}$. This is the dual multiplier corresponding to the solution ignoring all variable bounds, i.e., $x_i(\lambda) = (b_i\lambda + a_i)/d_i$ for all i . It resembles the initialization in the variable fixing method of Kiwiel [23]. Alternatively, if a primal estimate \bar{x} is provided, we assume that it conveys information about the bounds that are expected to be binding at the solution: variables reaching or violating their bounds in \bar{x} are expected to have active bounds at the solution. Hence, λ_0 is computed with $J = \{i \mid l_i < \bar{x}_i < u_i\}$. If this set is empty, we discard \bar{x} and set $J = \{1, 2, \dots, n\}$.

2.2 Variable fixing

As stated in [14], the Newton method can be combined with a variable fixing technique because φ is non-decreasing. In fact, x_i can be fixed to l_i if $\varphi(\lambda_k) > r$ and $x(\lambda_k)_i = l_i$. On the other hand, it can be fixed to u_i if $\varphi(\lambda_k) < r$ and $x(\lambda_k)_i = \bar{u}_i$. In the first case, the optimal $\lambda_* \leq \lambda_k$, while in the

second, $\lambda_* \geq \lambda_k$. This can reduce the number of operations in Algorithm 1, as fixed variables can be neglected in the computation of φ and its derivatives. It was verified in [14] that this can be effective in speeding up the method. In our implementation, we attempt to fix as many variables as possible before the secant step (line 18 of Algorithm 1).

This principle forms the basis of the variable fixing algorithms developed in [15, 22, 23] and references therein. These methods iteratively identify variables that are fixed at their bounds in the solution until the optimal set of free variables is determined, allowing the final solution to be computed using its associated multiplier estimate. In this work, we focus on Condat’s method for projection onto the simplex, as it is widely considered the most efficient variant available.

Projecting onto a simplex and Condat’s algorithm

Let us focus on solving (proj_Δ) . Variable fixing methods aim to identify the subset of free variables at the optimum. Given a tentative set of free variables $J \subseteq \{1, 2, \dots, n\}$, a candidate primal-dual pair can be computed using specialized versions of (4) and (1):

$$\lambda_J = \frac{r - \sum_{i \in J} y_i}{|J|}, \quad x_i^J = \max\{0, y_i + \lambda_J\}, \quad \forall i = 1, \dots, n. \quad (5)$$

Now, recalling that an optimal dual solution λ_* recovers the optimal primal solution x^* through (1), it follows that

$$\sum_{i=1}^n \max\{0, y_i + \lambda_*\} = \sum_{i=1}^n x_i^* = r = \sum_{i \in J} (y_i + \lambda_J) \leq \sum_{i=1}^n \max\{0, y_i + \lambda_J\} = \sum_{i=1}^n x_i^J.$$

Consequently, $\lambda_J \geq \lambda_*$.

This observation is the fundamental building block of variable fixing methods. The process begins by assuming that all variables are potentially free at the solution, i.e., $J = \{1, \dots, n\}$. The algorithm then verifies whether the associated x^J is feasible; if so, the problem is solved. Otherwise, one or more variables that must be fixed at 0, the lower bound, are identified, and the set J is reduced before starting a new iteration [22, 23].

Condat’s method to project onto simplex and ℓ_1 ball

In [15], Condat made a key observation that resulted in the most widely used algorithm for projection onto a simplex. He realized that as soon as a variable is identified as fixed, the set J and its respective multiplier estimate λ_J can be updated immediately within the same iteration, introducing a Gauss-Seidel flavor to the method. This approach leads directly to Algorithms 2 and 3.

Algorithm 2 constructs an initial candidate subset of free variables by adding one variable at a time, provided it cannot be proven that the variable must be fixed at 0 in the optimal solution. Algorithm 3 then refines this set by identifying further variables to fix. In both cases, the multiplier estimate is constantly updated in a Gauss-Seidel fashion.

3 A specialized Newton method to project onto a simplex

We now discuss the specialization of Algorithm 1 for solving (proj_Δ) , with the objective of deriving a method that is competitive with Condat’s algorithm. This problem is equivalent to (CQK) , up to a constant in the objective, by setting $D = I$, $a = y$ and $r > 0$, while taking $b_i = 1$, $l_i = 0$ and $u_i = +\infty$ for all i . The expressions (1)–(3) simplify accordingly. In the following, we demonstrate that with appropriate initialization, Algorithm 1 avoids vanishing derivatives. This property allows for a streamlined implementation, resulting in Algorithm 4.

Theorem 3.1. *Consider Algorithm 1 applied to (proj_Δ) . Suppose that $\lambda_0 \geq \underline{y} = \min_i \{-y_i\}$ is not a zero of $\varphi(\lambda) - r$. Then*

1. $\varphi'_+(\lambda_0) > 0$ and, if $\varphi(\lambda_0) > r$, $\varphi'_-(\lambda_0) > 0$;

Algorithm 2 Initialize λ (simplex projection)

Require: a subset of variable indices $I = \{i_1, \dots, i_p\} \subseteq \{1, \dots, n\}$.

- 1: Set $J \leftarrow \{i_1\}$, $\tilde{J} \leftarrow \emptyset$, $\lambda \leftarrow r - y_{i_1}$
 - 2: **for** $j = 2, \dots, p$ **do**
 - 3: **if** $y_{i_j} + \lambda > 0$ **then**
 - 4: Set $\lambda \leftarrow (r - \sum_{\ell \in J} y_{i_\ell} - y_{i_j}) / (|J| + 1)$
 - 5: **if** $\lambda < r - y_{i_j}$ **then**
 - 6: Update $J \leftarrow J \cup \{i_j\}$
 - 7: **else**
 - 8: set $\tilde{J} \leftarrow \tilde{J} \cup J$, $J \leftarrow \{i_j\}$ and $\lambda \leftarrow r - y_{i_j}$
 - 9: **for all** $j \in \tilde{J}$ **do**
 - 10: **if** $y_j + \lambda > 0$ **then**
 - 11: Set $\lambda \leftarrow (r - \sum_{\ell \in J} y_{i_\ell} - y_j) / (|J| + 1)$ and $J \leftarrow J \cup \{j\}$
 - 12: **return** the list of non-fixed variables $J \subseteq I$
-

Algorithm 3 Condat's method to project a point onto simplex

Require: the point y who wants to project

- 1: Compute λ and $J \subseteq \{1, \dots, n\}$ by Algorithm 2 with $I = \{1, \dots, n\}$
 - 2: **while** J changes **do**
 - 3: **for all** $j \in J$ **do**
 - 4: **if** $y_j + \lambda \leq 0$ **then**
 - 5: Set $J \leftarrow J \setminus \{j\}$ and update $\lambda \leftarrow \lambda - (y_j + \lambda) / |J|$
 - 6: **return** the solution x^* of (proj_Δ) defined by $x_i^* = \max\{0, y_i + \lambda\}$
-

2. For all $k \geq 0$, $\lambda_{k+1} = \tilde{\lambda}_k \in [\underline{\lambda}, \bar{\lambda}]$;
3. For all $k \geq 1$, $\lambda_k \geq \lambda_{k+1} \geq \lambda_* > \underline{y}$, where λ_* is the zero of $\varphi(\lambda) - r$;
4. For all $k \geq 1$, $\varphi(\lambda_k) > r$ and $\varphi'_-(\lambda_k) > 0$.

Proof. The only breakpoints in this case are $\underline{l}_i = -y_i$. From (2) and (3), we have $\varphi(\lambda) = \sum_{i=1}^n \max\{0, y_i + \lambda\}$, $\varphi'_+(\lambda) = \sum_{i \mid -y_i \leq \lambda} 1$ and $\varphi'_-(\lambda) = \sum_{i \mid -y_i < \lambda} 1$. Since $\lambda_0 \geq \underline{y}$, immediately $\varphi'_+(\lambda_0) > 0$. As $y_i + \underline{y} \leq 0$ for all i , we have $\varphi(\underline{y}) = 0 < r$. So, if $\varphi(\lambda_0) > r$, then $\lambda_0 > \underline{y}$, in which case $\varphi'_-(\lambda_0) > 0$. Item 1 follows.

At iteration $k = 0$, the Newtonian step $\tilde{\lambda}_k$ is accepted as the new iterate λ_1 since $\tilde{\lambda}_0 = \lambda_0 - (\varphi(\lambda_0) - r) / \varphi'_+(\lambda_0) \in (\underline{\lambda}, \bar{\lambda}) = (\lambda_0, \infty)$ if $\varphi(\lambda_0) < r$ and $\tilde{\lambda}_0 = \lambda_0 - (\varphi(\lambda_0) - r) / \varphi'_-(\lambda_0) \in (\underline{\lambda}, \bar{\lambda}) = (-\infty, \lambda_0)$ if $\varphi(\lambda_0) > r$. The fact that φ is convex and non-decreasing guarantees that $\varphi(\lambda_1) > r = \varphi(\lambda_*)$. This implies $\lambda_1 \geq \lambda_*$, and so $\varphi'_-(\lambda_1) > 0$. In the second iteration, $\underline{\lambda}$ remains unchanged, $\bar{\lambda} \leftarrow \lambda_1$ and $\lambda_2 = \tilde{\lambda}_1 = \lambda_1 - (\varphi(\lambda_1) - r) / \varphi'_-(\lambda_1) \in [\lambda_*, \lambda_1] \subseteq (\underline{\lambda}, \bar{\lambda})$. This repeats at every iteration, leading to items 2, 3 and 4. \square

3.1 Warm start and variable fixing

Let us now consider the computation of the initial multiplier λ_0 for Algorithm 4. If no prior information is available, one possibility is to use Algorithm 2 with $I = \{1, \dots, n\}$. Since this method refines the multiplier estimate using a Gauss-Seidel approach, it generally provides a better approximation than a direct application of formula (4). In particular, we know that Algorithm 2 is guaranteed to return $\lambda_0 \geq \lambda_* > \underline{y}$, which avoids the need for the verification performed in line 1 of the specialized Newton method. Moreover, this initialization identifies many variables that are fixed at 0 in the optimal solution, thereby reducing the problem size for the subsequent Newton iterations if variable fixing is employed.

On the other hand, there are scenarios where approximate primal solutions are readily available. This occurs, for example, when projections are performed within the inner iterations of an outer

Algorithm 4 Semi-smooth Newton method for solving (proj_Δ)

Require: the initial dual estimate λ_0

- 1: Check, if necessary, whether $\lambda_0 \geq \underline{y} = \min_i\{-y_i\}$ or not and update $\lambda_0 \leftarrow \max\{\lambda_0, \underline{y}\}$
 - 2: **if** $\varphi(\lambda_0) = r$ **then**
 - 3: Stop and return $x(\lambda_0)$ as the solution of (proj_Δ)
 - 4: **if** $\varphi(\lambda_0) < r$ **then**
 - 5: $\lambda_1 = \lambda_0 - \frac{\varphi(\lambda_0) - r}{\varphi'_+(\lambda_0)}$
 - 6: **else**
 - 7: $\lambda_1 = \lambda_0 - \frac{\varphi(\lambda_0) - r}{\varphi'_-(\lambda_0)}$
 - 8: Set $k \leftarrow 1$
 - 9: **if** $\varphi(\lambda_k) \leq r$ **then**
 - 10: Stop and return $x(\lambda_k)$ as the solution of (proj_Δ)
 - 11: Define $\lambda_{k+1} = \lambda_k - \frac{\varphi(\lambda_k) - r}{\varphi'_-(\lambda_k)}$, set $k \leftarrow k + 1$ and go to line 9
-

algorithm or when a sequence of closely related problems is solved. In these cases, the proximity of successive points allows the previous projection to serve as an estimate for the current one. This strategy was employed in [14] to accelerate the solution of SVM problems.

In the (proj_Δ) case, a warm start can be performed by using Algorithm 2 to estimate the initial multiplier. Let $\bar{x} \geq 0$ be a good approximation of the optimal solution $x^* = x(\lambda_*)$ of (proj_Δ) . We can then define the set of candidates for free variables as the support of the approximation, $\bar{I}_+ = \{i \mid \bar{x}_i > 0\}$, and use it as the initial set I in Algorithm 2. This approach assumes that the free variables in \bar{x} are likely to remain free in x^* , thereby yielding a more accurate λ_0 . This initialization maintains the property that $\lambda_0 \geq \lambda_* \geq \underline{y}$. Furthermore, we can fix $x_i^* = 0$ whenever $y_i + \lambda \leq 0$, where λ is the intermediate approximation computed during the execution of Algorithm 2 that leads to the final value λ_0 .

Finally, it is worth noting that we do not need to precompute \bar{I}_+ explicitly to apply Algorithm 2 with $I = \bar{I}_+$. This would require an additional pass over the data. Instead, we identify these indices by testing whether the corresponding component of \bar{x} is positive before updating λ (lines 4, 8, and 11 in Algorithm 2). In our implementation, we maintain an auxiliary set of indices J_+ to store the elements of I_+ used for computing the multiplier. In the rare event that $J_+ = \emptyset$, the estimate (5) is undefined. In this case, we simply set $\lambda = \max\{r/n, -y_1\} \geq \underline{y}$. We present numerical results illustrating the computational benefits of this warm-start strategy for Algorithm 4 in Section 5.2.2.

3.2 Projection onto a ℓ_1 ball

Clearly, if $y \in \mathcal{B}$, the projection of y onto \mathcal{B} is y itself. Otherwise, the projection can be recovered from projecting the entry-wise absolute value $|y| = (|y_1|, \dots, |y_n|)$ onto Δ and multiplying its result by the original signs of y , see [15, Proposition 2.1].

In this case, we can also derive a more aggressive variable fixing result. The next lemma, whose proof follows from [15, Proposition 2.1] and (1)–(3), establishes that the i -th coordinate of the optimal projection x_i^* is zero whenever $y_i = 0$ and $y \notin \mathcal{B}$. This allows us to specialize the variable fixing criterion used in the computation of λ_0 beyond that of Algorithm 2. Specifically, the conditions $y_{i_j} + \lambda > 0$ and $y_j + \lambda > 0$ in lines 3 and 10 to $\min\{|y_{i_j}|, |y_{i_j}| + \lambda\} > 0$ and $\min\{|y_j|, |y_j| + \lambda\} > 0$, respectively. Clearly, y_l must be changed to $|y_l|$ elsewhere in the logic.

Lemma 3.1. *Suppose that $\sum_{i=1}^n |y_i| \geq r$ and let $x^* = P_{\mathcal{B}}(y)$. Then, for all $i = 1, \dots, n$, $x_i^* = \text{sgn}(y_i)x(\lambda_*)_i = \text{sgn}(y_i) \max\{0, |y_i| + \lambda_*\}$, where $\lambda_* \leq 0$ solves the dual of (proj_Δ) with $|y|$ in place of y .*

4 Parallelizing CQK methods

As stated in the introduction, Dai and Chen recently proposed a parallelization strategy for simplex projection methods. They achieve this by exploiting the fact that for a subproblem containing only

a subset of the variables, if a variable is identified as fixed at 0, it necessarily remains fixed at 0 in the full problem instance [16, Proposition 4]. Parallelization is achieved by solving multiple subproblems, which partition the original instance, to a coarse precision to identify the majority of the fixed variables. Subsequently, a reduced version of the full instance is solved. Since the vast majority of variables are expected to be fixed in a typical solution, this final problem is usually very small and can be solved in a fraction of the time required by the initial parallel phase. This strategy can be applied to any method that performs variable fixing. In particular, it results in a very effective variant of Condat’s method, which was shown to be the fastest in their implementation. This efficiency is possible because the parallel phase, which identifies the fixed variables, occurs before the Gauss-Seidel-style loop in Algorithm 3, which is inherently difficult to parallelize.

On the other hand, the pure Newton methods, Algorithm 1 and 4, can be trivially parallelized in a Jacobi-like fashion, as their primary steps contain no sequential dependencies. The bulk of the computational effort is associated with evaluating φ and its derivatives. Such computation rely only on the current multiplier λ_k , which is a single scalar that can be efficiently shared among parallel workers. In fact, these methods fit naturally into a MapReduce framework [18]. The *map* phase involves computing the individual summands that define the value of φ and its derivatives across subsets of the data. The *reduce* phase then performs the summation to aggregate these values. Subsequently, a simple multiplier update is performed to initiate the next iteration. This makes such methods ideal for implementation on GPUs, where the memory indirection and control-flow complexities often associated with the variable-fixing logic can be difficult to implement efficiently.

CPU implementations of the method can still benefit from variable fixing. In this context, each worker in the MapReduce framework is responsible for a subset of the data (a *chunk*). At each iteration, the worker computes the partial summands of φ and its derivatives for the variables in its chunk and performs local variable fixing. This remains possible because all workers share a consistent multiplier estimate, which coordinates their local computations. In our implementation, we also incorporate a mechanism to merge chunks that become too small; this avoids the overhead of spawning or managing threads for tasks that involve too little computational work.

The initial multiplier λ_0 can also be computed in parallel. On GPUs or in the general (CQK) case, it is preferable to use the formula provided in (4), which fits naturally into a pure MapReduce framework without requiring memory indirection. Conversely, for the simplex case on CPUs, we can employ the more sophisticated Algorithm 2. In this case, each worker executes the algorithm in parallel on a distinct subset I of the variables. Upon completion, each thread will have identified its own subset J_I of non-fixed variables. The global λ_0 is then obtained via (5) using the union $J = \cup_I J_I$. This aggregation is performed using the partial sums already computed within each chunk, thereby avoiding redundant operations when calculating the final λ_0 .

Finally, the primal solution $x(\lambda_*)$ can also be computed in parallel, as it is fundamentally a *map* operation in the GPU implementation. In the CPU implementation, which utilizes variable fixing, this calculation is performed as soon as a variable is fixed. This is necessary because fixing a variable to its bound can modify the right-hand side of the equality constraint, r . However, in the specific case of the simplex, $x(\lambda_*)$ is calculated only at the end of the process; since fixed variables in the simplex are always zero, they do not affect the right-hand side of the constraint.

5 Numerical tests

We have implemented the Newton algorithms in a Julia package named `NewtonCQK.jl` that can be installed using the language’s standard package system. The code is available at <https://github.com/pjssilva/NewtonCQK>. It has both CPU (with variable fixing) and a GPU (pure MapReduce) variants to solve the general (CQK) problem and its special cases (`proj Δ`) and the associated projection on the ℓ_1 -ball.

The implementations of Algorithm 1 stop declaring success if one of the following criteria is satisfied:

1. $|\varphi(\lambda_k) - r| < \epsilon^{3/4} \left(\sum_{i=1}^n |b_i x(\lambda_k)| + |r| \right)$ (relative to line 2 of Algorithm 1);
2. $|(\varphi(\lambda_k) - r)/\varphi'(\lambda_k)| < \epsilon^{3/4}$ or $\lambda_{k-1} = \lambda_k$ (numerically zero step);

Table 1: Hardware specification.

	CPU	GPU
Model	AMD EPYC 9254 24-Core	NVIDIA Tesla A100
Cores	48 divided into 2 equal processors	6,912 Cuda cores
Cache	L1: 96 KB, L2: 512 KB/core; L3: 32 MB	–
TFLOPS (FP64)	$\approx 1.3 - 1.6$ TFLOPS	≈ 9.7 TFLOPS
Memory	1.5 TB DDR5	40 GB HBM2
Mem. bandwidth	≈ 460.8 GB/s	≈ 1.56 TB/s

$$3. \bar{\lambda} - \underline{\lambda} < \epsilon^{3/4} \max\{|\bar{\lambda}|, |\underline{\lambda}|\} \quad (\text{no improvement is expected}),$$

where ϵ is the machine epsilon ($\epsilon \approx 2.22 \times 10^{-16}$ for 64-bit floating point and $\epsilon \approx 1.19 \times 10^{-7}$ for 32-bit). Criteria **1** and **3** appear in the implementation in [14], except for the use of 10^{-12} in item **1** and 2.22×10^{-16} in item **3** instead of $\epsilon^{3/4}$. For Algorithm 4 and related, only criteria **2** and **3** are used.

We test our implementation against the following software:

- the sequential Newton method described in [14] for solving (CQK). Its C code is freely available at www.ime.unicamp.br/~pjssilva/code. We modified the code to use the stopping criteria described above. We refer to this implementation as the “CMS” for short;
- the sequential Condat’s method (Algorithm 3) for projecting onto simplex, whose C code is freely available at [lcondat.github.io/software.html](https://github.com/lcondat/software.html);
- the parallel Condat’s method developed by Dai and Chen [16] for projecting onto simplex and ℓ_1 ball, whose Julia code is freely available at github.com/foreverdyz/Parallel-Simplex-Projection.

All methods use a similar amount of memory, the additional memory required for the parallel variations is at most proportional to the number of cores, which is negligible when compared with problem sizes. Hence we focus the comparison on running time. The CPU implementations were tested on a computer equipped with two 24 core AMD EPYC 9254, totalizing 48 cores, and 1.5 TB RAM under Debian 6.1. Experiments with GPU were performed on another computer using an NVIDIA Tesla A100 40GB. Table 1 presents the detailed hardware specification.

Let us define the nomenclature used in the following sections. When comparing different methods or distinct implementations of the same algorithm, we designate a base method and report the *relative performance* of alternative methods. We define *relative performance* as the ratio of the execution time of the sequential base method to that of an alternative (possibly parallel) implementation. Consequently, a value greater than 1 indicates that the alternative is faster, while a value less than 1 indicates that the base method is more efficient. We utilize the term (parallel) *speedup* to assess how implementations scale with the number of processing units. By using a single sequential method as the common numerator for these ratios, we can compare the absolute performance of different algorithms and their respective parallel behaviors within the same figure. An increasing ratio indicates effective parallelization, while a decrease suggests that computational overhead – likely due to thread management or communication bottlenecks – outweighs the gains from concurrent execution.

5.1 Tests with general quadratic knapsack problems

5.1.1 Randomly generate instances

Following [14] and references therein, we considered three classes of problems:

1. *Uncorrelated*: $d_i, a_i, b_i \sim U[10, 25]$ for each i ;
2. *Weakly correlated*: $b_i \sim U[10, 25]$ and $d_i, a_i \sim U[b_i - 5, b_i + 5]$ for each i ;
3. *Correlated*: $b_i \sim U[10, 25]$ and $d_i = a_i = b_i + 5$ for each i ,

where $U[p, q]$ stands for the uniform distribution in the interval $[p, q]$. For all classes, l_i, u_i 's were chosen as the minimum and maximum between two numbers sorted i.i.d. from $U[10, 25]$, and $r \sim U[b^t l, b^t u]$. The random numbers were generated using the Julia package `Distributions.jl` [4]. In particular we used its default option, the algorithm `Xoshiro256++` [25].

We generated 20 instances for dimensions ranging from 1,000 to 1,000,000,000. The runtime for each instance was measured using `BenchmarkTools.jl` [12] to minimize measurements errors. In particular `BenchmarkTools.jl` was set to solve each instance until 10,000 runs or 2 seconds had elapsed. The final value for an instance is the minimal measured runtime as it is a robust estimator of the actual value [12]. We then report for each dimension the median runtime of its instances.

Table 2 presents the median CPU times for the Julia implementation of Algorithm 1 with variable fixing present in `NewtonCQK.jl` alongside the original CMS implementation written in C. Across various problem classes and sizes, the results demonstrate that the Julia version is nearly as fast as its C counterpart, requiring at most 10% more time for small instances. Notably, this performance gap narrows as the problem size increases. This slight disparity should not be attributed to the programming language alone; rather, it reflects different architectural choices. Our Julia version utilizes the MapReduce framework provided by `OhMyThreads.jl` [2], which allows the same codebase to execute in a multi-threaded environment and exploit the multiple cores of modern CPUs. This parallelization capability is not available in the original serial CMS implementation. The Julia code can also work with any floating-point type and performs basic sanity tests on data (check whether $d > 0$, $b > 0$ and $l \leq u$) that is not present in the CMS implementation.

n	Uncorrelated		Weakly correlated		Correlated	
	CMS time (ms)	<code>NewtonCQK.jl</code> relative	CMS time (ms)	<code>NewtonCQK.jl</code> relative	CMS time(ms)	<code>NewtonCQK.jl</code> relative
10^3	6.22e-03	1.0983	6.47e-03	1.0604	7.33e-03	1.0745
10^4	6.44e-02	1.0800	6.74e-02	1.0888	7.53e-02	1.0610
10^5	3.51e+00	1.0589	3.36e+00	1.0799	3.05e+00	1.0883
10^6	3.89e+01	1.0541	3.50e+01	1.0611	3.15e+01	1.0723
10^7	3.99e+02	1.0304	3.67e+02	1.0216	3.26e+02	1.0504
10^8	3.67e+03	1.0366	3.62e+03	1.0403	3.32e+03	1.0474
10^9	4.22e+04	1.0079	3.63e+04	1.0398	3.32e+04	1.0472

Table 2: Comparison between the sequential Algorithm 1 implemented in Julia and the CMS implementation for a single core. Times are in milliseconds and were taken as the median over the 20 generated instances. The columns labeled “relative” present the ratio between the time used by our implementation and the CMS value.

Next, we focus on the parallel scalability of the `NewtonCQK.jl` implementation of Algorithm 1 with variable fixing on CPUs. Figure 2 illustrates the speedup relative to the sequential version as the problem size increases. As expected, employing multiple threads is not effective for small problems ($n \leq 10,000$). In these cases, thread management overhead constitutes a significant portion of the total execution time. Generally, as the number of variables increases, the benefits of using additional threads become more pronounced, with the speedup approaching linearity for the largest instances. In our benchmarks, parallel execution becomes beneficial for $n \geq 100,000$. Ultimately, users should select the threading configuration that best aligns with their specific problem scale and hardware architecture.

Finally, we compare the CPU and GPU variants. It is important to note that the GPU version does not utilize variable fixing. Table 3 presents these results, where the GPU columns indicate the relative performance of the GPU version compared to the CPU implementation using various thread counts. The values in parentheses represent the mean number of iterations performed across the 20 generated instances. Instances with $n = 10^9$ were omitted due to GPU memory constraints. For large-scale problems ($n \geq 10^6$), the GPU version is significantly faster, outperforming even the CPU implementation running on all 48 threads. Notably, for the largest problems ($n = 10^8$), the CPU version using a single thread and 48 threads is at least 151 and 6.8 times slower than the GPU implementation, respectively.

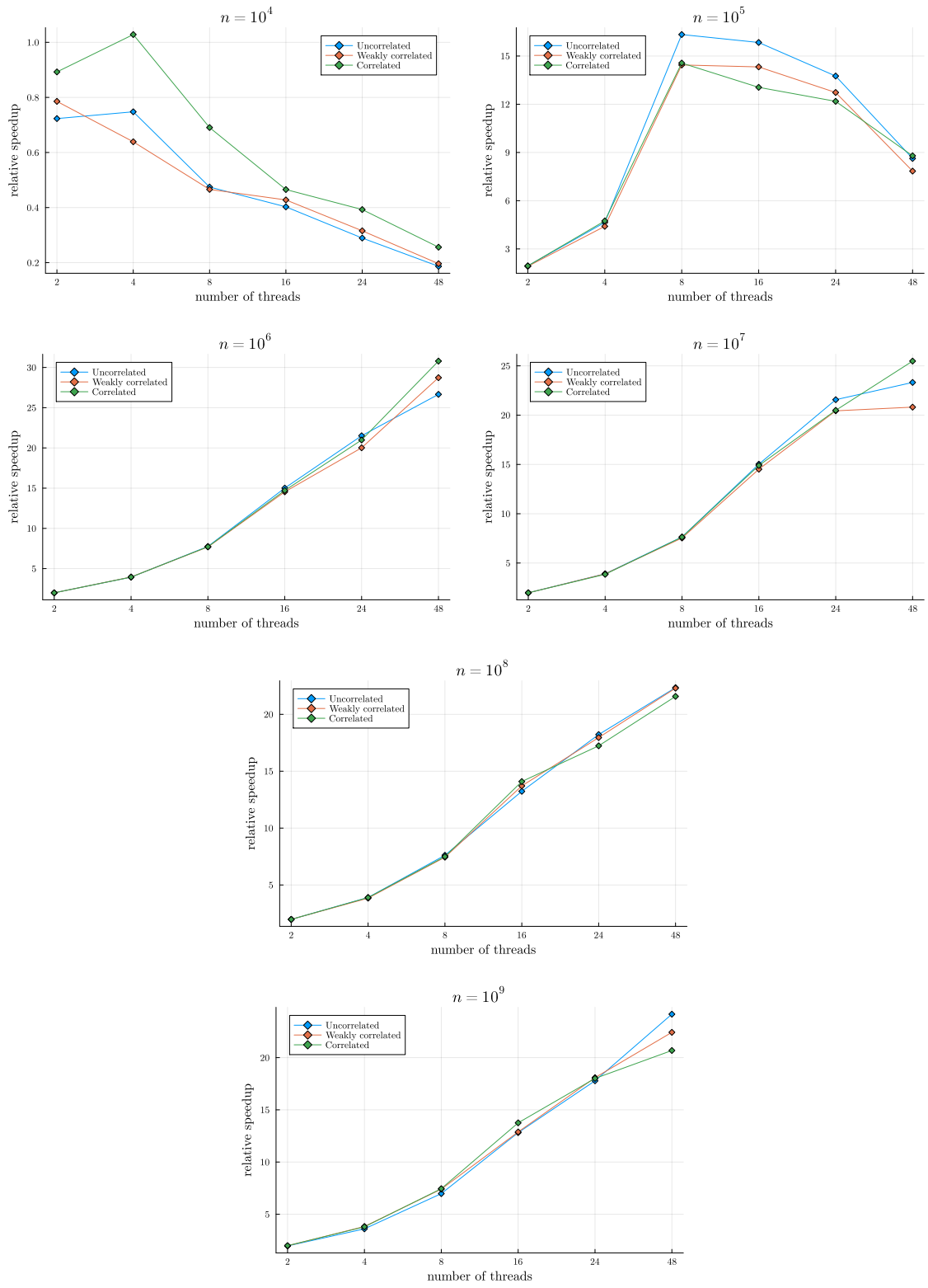


Figure 2: Speedups of parallel Algorithm 1 with variable fixing relative to the sequential version on random instances.

n	th	Uncorrelated		Weakly correlated		Correlated	
		CPU time (ms)	GPU relative	CPU time (ms)	GPU relative	CPU time (ms)	GPU relative
10^4	1	7e-02 (6.6)	0.1 (5.7)	7e-02 (5.6)	0.1 (5.5)	8e-02 (5.3)	0.2 (5.7)
10^4	2	1e-01 (6.6)	0.2 (5.7)	9e-02 (5.6)	0.2 (5.5)	9e-02 (5.3)	0.2 (5.7)
10^4	4	9e-02 (6.6)	0.2 (5.7)	1e-01 (5.6)	0.2 (5.5)	8e-02 (5.3)	0.2 (5.7)
10^4	8	1e-01 (6.6)	0.3 (5.7)	2e-01 (5.6)	0.3 (5.5)	1e-01 (5.3)	0.2 (5.7)
10^4	16	2e-01 (6.6)	0.3 (5.7)	2e-01 (5.6)	0.3 (5.5)	2e-01 (5.3)	0.3 (5.7)
10^4	24	2e-01 (6.6)	0.4 (5.7)	2e-01 (5.6)	0.5 (5.5)	2e-01 (5.3)	0.4 (5.7)
10^4	48	4e-01 (6.6)	0.7 (5.7)	4e-01 (5.6)	0.8 (5.5)	3e-01 (5.3)	0.6 (5.7)
10^5	1	4e+00 (5.5)	5.6 (6.3)	4e+00 (6.5)	5.5 (6.0)	3e+00 (5.6)	4.9 (6.0)
10^5	2	2e+00 (5.5)	2.9 (6.3)	2e+00 (6.5)	2.9 (6.0)	2e+00 (5.6)	2.5 (6.0)
10^5	4	8e-01 (5.5)	1.2 (6.3)	8e-01 (6.5)	1.2 (6.0)	7e-01 (5.6)	1.0 (6.0)
10^5	8	2e-01 (5.5)	0.3 (6.3)	3e-01 (6.5)	0.4 (6.0)	2e-01 (5.6)	0.3 (6.0)
10^5	16	2e-01 (5.5)	0.4 (6.3)	3e-01 (6.5)	0.4 (6.0)	3e-01 (5.6)	0.4 (6.0)
10^5	24	3e-01 (5.5)	0.4 (6.3)	3e-01 (6.5)	0.4 (6.0)	3e-01 (5.6)	0.4 (6.0)
10^5	48	4e-01 (5.5)	0.6 (6.3)	5e-01 (6.5)	0.7 (6.0)	4e-01 (5.6)	0.6 (6.0)
10^6	1	4e+01 (6.1)	48.2 (6.1)	4e+01 (6.4)	50.5 (5.5)	3e+01 (5.5)	45.7 (5.7)
10^6	2	2e+01 (6.1)	24.2 (6.1)	2e+01 (6.4)	25.4 (5.5)	2e+01 (5.5)	23.0 (5.7)
10^6	4	1e+01 (6.1)	12.2 (6.1)	9e+00 (6.4)	12.8 (5.5)	9e+00 (5.5)	11.6 (5.7)
10^6	8	5e+00 (6.1)	6.2 (6.1)	5e+00 (6.4)	6.6 (5.5)	4e+00 (5.5)	5.9 (5.7)
10^6	16	3e+00 (6.1)	3.2 (6.1)	3e+00 (6.4)	3.5 (5.5)	2e+00 (5.5)	3.1 (5.7)
10^6	24	2e+00 (6.1)	2.2 (6.1)	2e+00 (6.4)	2.5 (5.5)	2e+00 (5.5)	2.2 (5.7)
10^6	48	2e+00 (6.1)	1.8 (6.1)	1e+00 (6.4)	1.8 (5.5)	1e+00 (5.5)	1.5 (5.7)
10^7	1	4e+02 (5.8)	145.6 (6.0)	4e+02 (6.2)	133.4 (5.8)	3e+02 (5.7)	122.3 (5.6)
10^7	2	2e+02 (5.8)	73.6 (6.0)	2e+02 (6.2)	67.5 (5.8)	2e+02 (5.7)	61.8 (5.6)
10^7	4	1e+02 (5.8)	37.2 (6.0)	1e+02 (6.2)	34.2 (5.8)	9e+01 (5.7)	31.7 (5.6)
10^7	8	5e+01 (5.8)	19.0 (6.0)	5e+01 (6.2)	17.7 (5.8)	4e+01 (5.7)	16.0 (5.6)
10^7	16	3e+01 (5.8)	9.7 (6.0)	3e+01 (6.2)	9.2 (5.8)	2e+01 (5.7)	8.2 (5.6)
10^7	24	2e+01 (5.8)	6.7 (6.0)	2e+01 (6.2)	6.5 (5.8)	2e+01 (5.7)	6.0 (5.6)
10^7	48	2e+01 (5.8)	6.2 (6.0)	2e+01 (6.2)	6.4 (5.8)	1e+01 (5.7)	4.8 (5.6)
10^8	1	4e+03 (6.0)	174.3 (5.9)	4e+03 (6.0)	151.1 (6.6)	3e+03 (6.0)	185.6 (5.6)
10^8	2	2e+03 (6.0)	88.3 (5.9)	2e+03 (6.0)	76.4 (6.6)	2e+03 (6.0)	94.0 (5.6)
10^8	4	1e+03 (6.0)	44.7 (5.9)	1e+03 (6.0)	39.3 (6.6)	9e+02 (6.0)	47.7 (5.6)
10^8	8	5e+02 (6.0)	22.9 (5.9)	5e+02 (6.0)	20.3 (6.6)	5e+02 (6.0)	24.8 (5.6)
10^8	16	3e+02 (6.0)	13.2 (5.9)	3e+02 (6.0)	11.0 (6.6)	2e+02 (6.0)	13.2 (5.6)
10^8	24	2e+02 (6.0)	9.6 (5.9)	2e+02 (6.0)	8.4 (6.6)	2e+02 (6.0)	10.8 (5.6)
10^8	48	2e+02 (6.0)	7.8 (5.9)	2e+02 (6.0)	6.8 (6.6)	2e+02 (6.0)	8.6 (5.6)

Table 3: Comparison between CPU and GPU versions of Algorithm 1 implemented in NewtonCQK.jl using 64 bit floating-point. Times are in milliseconds, and were taken as the median over the 20 generated instances. The values between parentheses are the mean of iterations.

5.1.2 Support vector machines

Following [14], we also evaluated our methods on non-synthetic datasets by solving soft-margin SVM binary classification problems. In this context, CQK subproblems arise naturally when applying projected gradient methods to solve the dual formulation of the SVM. A brief description of this setting follows.

Given a set of labeled data

$$T = \{(z^i, y_i) \mid z^i \in \mathbb{R}^m, y_i \in \{-1, 1\}, i = 1, \dots, n\}$$

we seek a classification function $F : \mathbb{R}^m \rightarrow \{-1, 1\}$ of the form

$$F(z) = \text{sgn} \left(\sum_{i=1}^n x_i^* y_i K(z, z^i) + b_* \right),$$

where $x^* \in \mathbb{R}^n$ and $b_* \in \mathbb{R}$ are the optimal parameters to be determined, and $K : \mathbb{R}^m \times \mathbb{R}^m \rightarrow \mathbb{R}$ is a fixed kernel function. In our experiments, we employ the standard Gaussian kernel $K(p, q) = \exp(-\gamma \|p - q\|^2)$, where $\gamma > 0$ is a specified hyperparameter.

The vector x^* is a solution to the dual problem [11]

$$\min_x f(x) = \frac{1}{2} x^t H x - e^t x \quad \text{s.t.} \quad y^t x = 0, \quad 0 \leq x \leq C e,$$

where e is a vector of ones, $C > 0$ is a hyperparameter, and H is the $n \times n$ symmetric matrix with entries $H_{ij} = y_i y_j K(z^i, z^j)$. Since H is not diagonal, the problem above is not in the form of (CQK). However, a projected gradient-type iteration

$$x^{k+1} = x^k + t_k d^k, \quad d^k = P_\Omega(x^k - \lambda_k \nabla f(x^k)) - x^k, \quad (6)$$

where $t_k, \lambda_k > 0$ and $\Omega = \{x \in \mathbb{R}^n \mid y^t x = 0, 0 \leq x \leq Ce\}$, requires computing the projection of $x^k - \lambda_k \nabla f(x^k)$ onto Ω . This corresponds exactly to solving the CQK subproblem

$$\min_x \frac{1}{2} x^t I x - (x^k - \lambda_k \nabla f(x^k))^t x \quad \text{s.t.} \quad y^t x = 0, \quad 0 \leq x \leq Ce. \quad (7)$$

The gradient-type method employed in our experiments is the Spectral Projected Gradient (SPG) method [6, 5]. This method was selected due to its excellent practical performance in solving large-scale constrained problems. The stopping criterion is defined by the infinity norm of the projected gradient at a given iterate being smaller than 10^{-4} .

Following the approach in [14], this section primarily aims to verify if utilizing the previous iterate x^k to warm start Algorithm 1 yields significant performance gains, as discussed in Section 3.1. Additionally, we investigate the behavior and efficiency of the parallel implementations in this practical application context.

For these experiments, we utilized two datasets:

1. The MNIST dataset of handwritten digits, as previously used in [14]. We selected all 5,851 training samples labeled as digit 8 and the first 5,851 occurrences of other digits, totaling 11,702 samples. The objective is to design a classifier F to determine whether a 20×20 pixel image represents the digit 8;
2. The Diabetes Health Indicators dataset from the U.S. Centers for Disease Control and Prevention (“cdc_diabetes”), which contains health and lifestyle information for 253,680 individuals. Following a similar sampling strategy, we selected the first 10,000 occurrences of “prediabetes or diabetes” and the first 10,000 occurrences of “no diabetes”, resulting in a total of 20,000 samples.

The datasets were obtained using the Julia package `OpenML.jl` (<https://github.com/JuliaAI/OpenML.jl>) under IDs 554 and 46,598, respectively. Detailed descriptions are available at <https://www.openml.org>.

Regarding the hyperparameters, we set $\gamma = 0.007$ and $C = 5.0$ for the MNIST dataset, and $\gamma = 0.5$ and $C = 10.0$ for `cdc_diabetes`. These values were obtained using cross validation and yield high-accuracy models on the training data, with a misclassification rate of less than 0.5%.

Figure 3 illustrates the relative performance of the `NewtonCQK.jl` and CMS implementations of Algorithm 1 with variable fixing and warm start, compared to the `NewtonCQK.jl` implementation without warm start (initialized according to (4)). The figure depicts the behavior over the first and last 100 SPG iterations, omitting the initial three iterations due to highly discrepant values. We observe that using x^k as the initial guess significantly improves performance, especially during the final iterations. As discussed in Section 3.1, this is expected because the subproblems (7) undergo only minor adjustments; thus, the set $\{i \mid 0 < x_i^k < C\}$ used to compute λ_0 remains mostly constant, identifying the active set at the solution. Our results corroborate the findings in [14]. Finally, `NewtonCQK.jl` and CMS exhibit similar behavior, as they implement essentially the same method, though results for the smaller MNIST instance confirm that the CMS implementation is slightly more efficient.

To conclude this subsection, we present the speedup of the parallel implementation in `NewtonCQK.jl` in Figure 4. In this context, multithreading proves beneficial only for a modest number of threads – specifically up to 4 for both datasets – given their relatively small scale. It is also important to emphasize that the initial multiplier λ_0 computed from (4) is identical in both the multithreaded and sequential implementations. This consistency contrasts with the projections onto the simplex and ℓ_1 -ball, which we address in the following subsections.

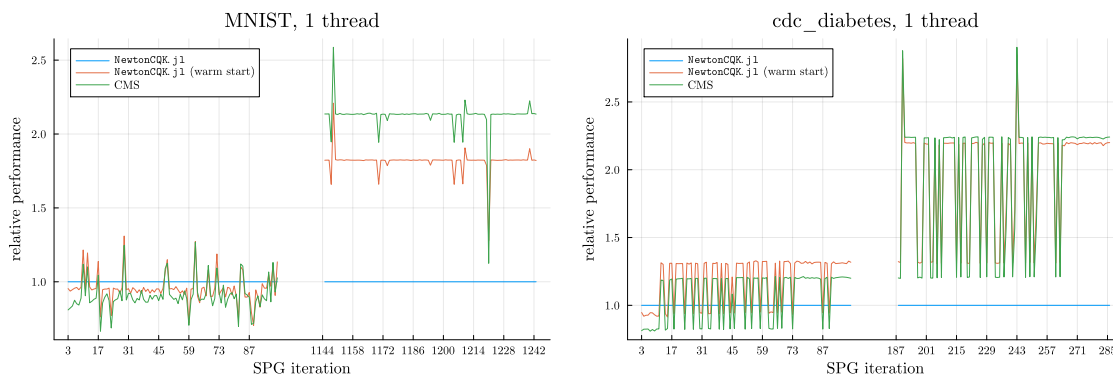


Figure 3: Relative performance of Algorithm 1 from `NewtonCQK.jl` and CMS using variable fixing and warm starts to solve (7) along the SPG iterations. The baseline (horizontal blue line at 1) is the performance of the `NewtonCQK.jl` without warm start.

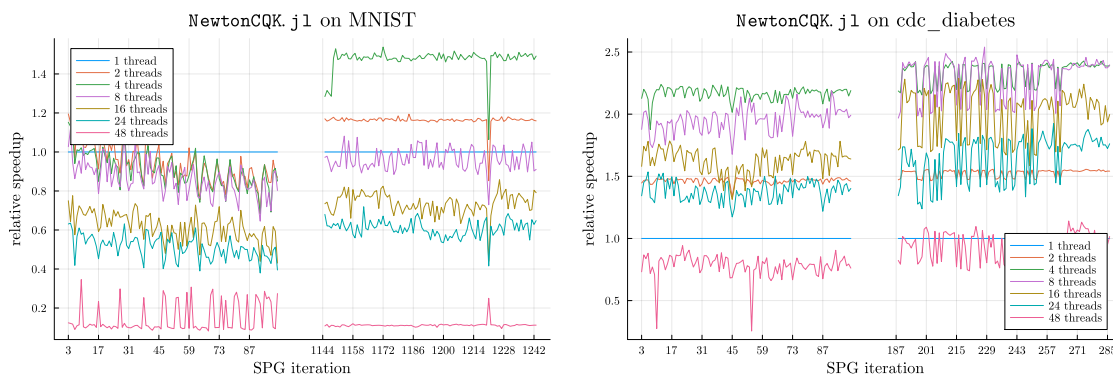


Figure 4: Speedups of parallel Algorithm 1 for solving (7) in relation to the sequential algorithm. All algorithms were executed using the current SPG iterate as warm start.

5.2 Projection onto simplex and ℓ_1 ball

5.2.1 Randomly generate instances

In this section, we present numerical results for problem (`proj Δ`). Following the methodology in [16] and references therein, we consider three classes of test problems based on the distribution of the components of y :

1. $y_i \sim U(0, 1)$ for each i ;
2. $y_i \sim N(0, 1)$, the standard normal distribution;
3. $y_i \sim N(0, 10^{-3})$ for each i .

As in the previous experiments, the problem dimension n ranges from 10^3 to 10^9 , with 20 instances generated for each configuration. In the rare event that a value $y_i = 0$ is generated, the entire instance is randomized again.

We compare below the implementation of Algorithm 4 from `NewtonCQK.jl` with Condat's original implementation of his method and with the implementation by Dai and Chen, which also features a parallel variant. It is important to point out that Condat's implementation returns a dense vector as the solution, even when the majority of its entries are zero (at the lower bound). In contrast, Dai and Chen exploit the expected sparsity of the solution to avoid allocating and filling

a large dense vector, returning a sparse representation instead. The `NewtonCQK.jl` implementation allows the user to specify the desired return type, hence we present results for both options.

Figures 5 and 6 present the speedup results for problem types 1 and 3 with $n \geq 10^4$; results for type 2 are omitted as they are qualitatively similar to those of type 1. Condat’s method serves as the baseline for all comparisons. By including results for the sequential implementations (running on a single thread) within these figures, we facilitate a direct comparison of the algorithmic efficiency of each method on a single core alongside their parallel scaling behavior.

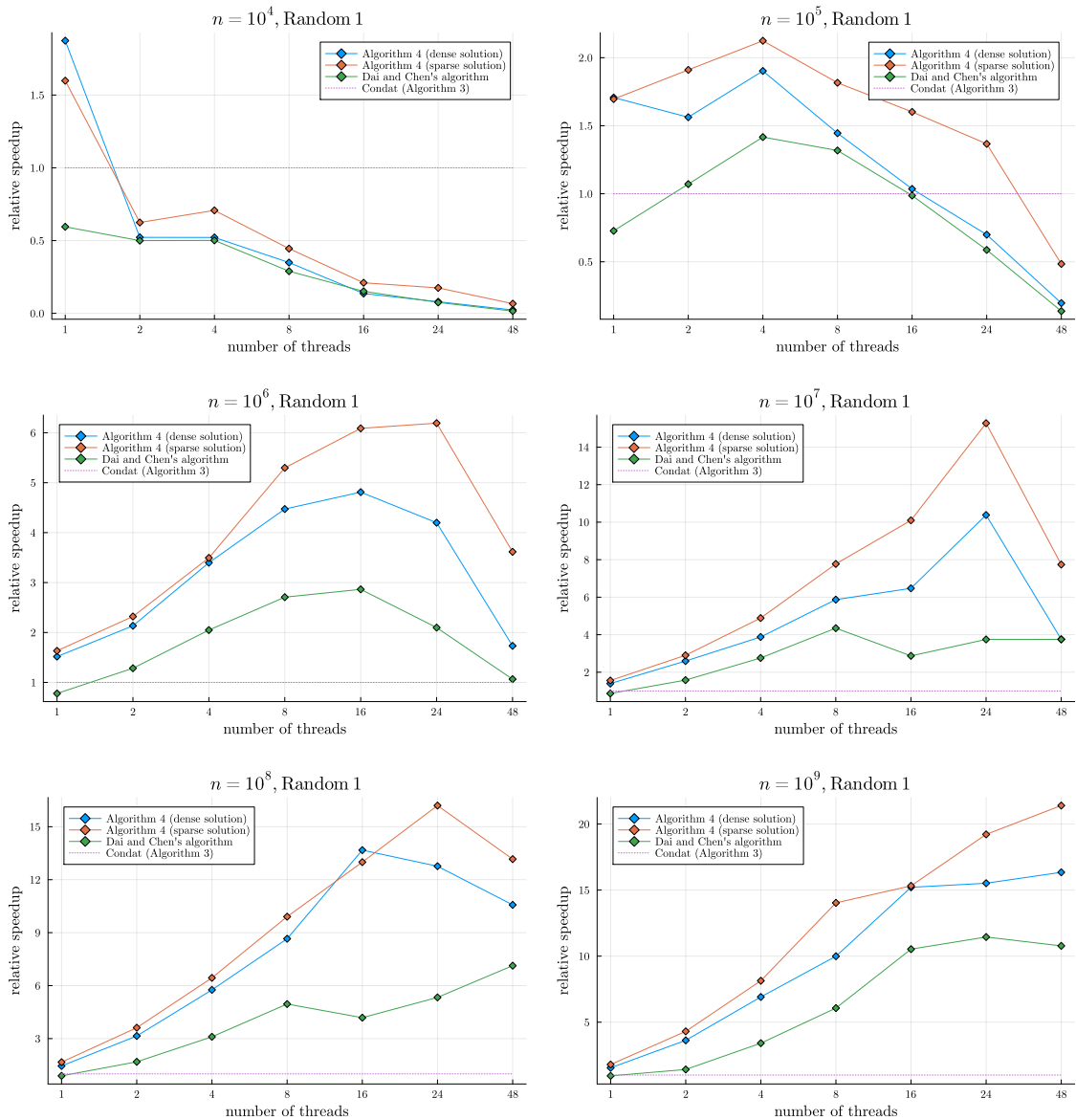


Figure 5: Speedups of Algorithm 4 implemented in `NewtonCQK.jl` (CPU versions returning dense and sparse solutions), Dai and Chen’s (sparse solution) and Condat’s (dense solution) algorithms on (`proj Δ`), instances of type 1. The base algorithm is of Condat, which is represented by the horizontal line.

We observe that both `NewtonCQK.jl` implementations of Algorithm 4 (dense and sparse output) outperforms Condat’s original C implementation even in single-threaded mode. Regarding parallel performance, we again observe no significant gains for small-scale problems ($n \leq 10^4$). For larger instances, the speedups achieved by the `NewtonCQK.jl` variant returning sparse vectors

are consistently higher than those attained by Dai and Chen’s algorithm. Notably, even the `NewtonCQK.jl` variant that produces dense vectors outperforms Dai and Chen’s method on large-scale problems. For $n \geq 10^8$, the performance improvement when increasing the thread count from 16 to 24 is less pronounced. This suggests that for very large problem sizes, the parallel workers may be reaching a point of diminishing returns, where computational overhead and memory access patterns become the primary limiting factors.

It is important to emphasize that the performance advantages demonstrated by the `NewtonCQK.jl` implementation stem not only from algorithmic differences – specifically the pure Newton approach versus variable fixing – but also from strategic choices in the data structures used to represent free variables. Condat’s and Dai and Chen’s methods maintain the y_i values of the unfixed variables throughout the iterations. In contrast, `NewtonCQK.jl`, following the logic of the CMS code for the general problem (CQK), tracks the indices of the free variables instead. The former approach is advantageous for maintaining data compactness in memory during the iterative process; however, it incurs a computational penalty at the conclusion, as a full scan of the problem data is required to construct the final output. The latter approach may result in more dispersed memory access during iterations, but it retains explicit knowledge of the few potentially non-zero values at the solution, thereby avoiding a costly final full scan.

Finally, Table 4 presents the results for the GPU MapReduce implementation of Algorithm 4. We recall that due to architectural constraints, this implementation utilizes the standard multiplier initialization derived from (4) and cannot incorporate the algorithmic refinements described in Section 3. Consequently, the GPU only consistently outperforms the single-threaded CPU implementation once the problem size reaches $n \geq 10^7$. Even in these instances, the gains are modest; the GPU version is at most six times faster than the single-threaded CPU implementation and never matches the performance of the 8-threaded CPU version. A key factor in this behavior is the iteration count: the GPU version can require up to five times more iterations than the Newton method using the initialization in Algorithm 2, with the discrepancy increasing for larger problems. This further demonstrates the effectiveness of the alternative multiplier initialization introduced by Condat. Nevertheless, a GPU implementation remains highly valuable for integration into workflows that reside entirely on the GPU, as it eliminates costly data transfers between the GPU and CPU, as seen in [3].

5.2.2 Basis pursuit

Let $A \in \mathbb{R}^{m \times n}$ be a matrix and a threshold $r > 0$. The basis pursuit denoising problem [13], or LASSO [31], has its alternative constrained formulation given by

$$\min_x \frac{1}{2} \|Ax - b\|^2 \quad \text{s.t.} \quad \|x\|_1 \leq r. \quad (8)$$

As in Section 5.1.2, we employ the SPG method to solve this problem. Each SPG iteration k requires computing a projection onto the ℓ_1 -ball, defined by the subproblem

$$\min_x \frac{1}{2} \|x - [x^k - \alpha_k A^t(Ax^k - b)]\|^2 \quad \text{s.t.} \quad \|x\|_1 \leq r, \quad (9)$$

where α_k is the spectral step size, see (6). The algorithm is initialized at the origin, $x^0 = 0$. The iterations terminate when the infinity norm of the projected gradient falls below the tolerance 10^{-4} .

We select two matrices from the collection compiled in [24, Table 3]: SC_1 ($m = 32,768$; $n = 65,536$) and SC_{11} ($m = 800$; $n = 88,119$), along with their provided right-hand sides b . We set the radius r to 6,717 and 34, respectively. These are the smallest integer values for which SPG returns a point whose residual of the linear system $Ax = b$ has Euclidean norm smaller than 10^{-2} . Such choice leads to a sparse solution for the SC_{11} instance, but not for SC_1 . This difference unveils distinct behaviors of the warm-start strategy, as discussed below. Our analysis focuses on the performance gains achieved by using x^k as the initial guess (warm start) in the specialized Algorithm 1 for solving the projection subproblem, as well as the potential benefits of parallelization.

Figure 7 illustrates the relative performance of the sequential algorithms, using the `NewtonCQK.jl` implementation without warm start as the baseline. As in previous cases, we

n	th	Random 1		Random 2		Random 3	
		CPU time (ms)	GPU relative	CPU time (ms)	GPU relative	CPU time (ms)	GPU relative
10^3	1	1e-03 (5.0)	0.0 (8.2)	7e-04 (2.5)	0.0 (9.2)	3e-03 (3.1)	0.0 (4.5)
10^3	2	2e-02 (5.3)	0.0 (8.2)	2e-02 (3.4)	0.0 (9.2)	3e-02 (3.3)	0.1 (4.5)
10^3	4	2e-02 (5.7)	0.0 (8.2)	2e-02 (4.3)	0.0 (9.2)	4e-02 (3.4)	0.1 (4.5)
10^3	8	5e-02 (6.0)	0.1 (8.2)	4e-02 (5.2)	0.1 (9.2)	7e-02 (3.4)	0.2 (4.5)
10^3	16	1e-01 (6.2)	0.2 (8.2)	8e-02 (5.5)	0.2 (9.2)	1e-01 (3.4)	0.4 (4.5)
10^3	24	2e-01 (6.3)	0.4 (8.2)	2e-01 (6.0)	0.3 (9.2)	2e-01 (3.4)	0.7 (4.5)
10^3	48	6e-01 (6.8)	1.2 (8.2)	5e-01 (6.5)	1.0 (9.2)	6e-01 (3.4)	2.0 (4.5)
10^4	1	7e-03 (5.8)	0.0 (10.1)	6e-03 (3.5)	0.0 (11.7)	2e-02 (5.0)	0.0 (7.0)
10^4	2	3e-02 (6.1)	0.0 (10.1)	2e-02 (4.2)	0.0 (11.7)	7e-02 (5.3)	0.1 (7.0)
10^4	4	3e-02 (6.3)	0.0 (10.1)	2e-02 (5.1)	0.0 (11.7)	8e-02 (5.8)	0.1 (7.0)
10^4	8	4e-02 (6.9)	0.0 (10.1)	4e-02 (5.7)	0.0 (11.7)	1e-01 (6.0)	0.1 (7.0)
10^4	16	1e-01 (7.1)	0.1 (10.1)	8e-02 (6.2)	0.1 (11.7)	2e-01 (6.0)	0.2 (7.0)
10^4	24	2e-01 (7.2)	0.2 (10.1)	2e-01 (6.6)	0.1 (11.7)	2e-01 (6.0)	0.4 (7.0)
10^4	48	6e-01 (7.8)	0.7 (10.1)	5e-01 (7.2)	0.5 (11.7)	6e-01 (6.0)	1.0 (7.0)
10^5	1	7e-02 (6.8)	0.1 (12.1)	6e-02 (3.0)	0.0 (14.0)	1e-01 (6.3)	0.1 (9.1)
10^5	2	8e-02 (7.0)	0.1 (12.1)	4e-02 (4.5)	0.0 (14.0)	1e-01 (6.9)	0.2 (9.1)
10^5	4	7e-02 (7.3)	0.1 (12.1)	3e-02 (5.5)	0.0 (14.0)	1e-01 (7.0)	0.2 (9.1)
10^5	8	9e-02 (7.8)	0.1 (12.1)	5e-02 (6.0)	0.0 (14.0)	2e-01 (7.2)	0.2 (9.1)
10^5	16	1e-01 (8.1)	0.1 (12.1)	9e-02 (6.7)	0.1 (14.0)	2e-01 (7.7)	0.2 (9.1)
10^5	24	2e-01 (8.2)	0.2 (12.1)	1e-01 (7.0)	0.1 (14.0)	2e-01 (7.9)	0.3 (9.1)
10^5	48	7e-01 (8.6)	0.7 (12.1)	5e-01 (7.7)	0.4 (14.0)	7e-01 (8.0)	0.9 (9.1)
10^6	1	8e-01 (7.7)	0.6 (14.0)	6e-01 (3.8)	0.4 (16.4)	2e+00 (7.7)	1.9 (11.6)
10^6	2	5e-01 (8.0)	0.4 (14.0)	2e-01 (4.9)	0.2 (16.4)	2e+00 (8.0)	1.4 (11.6)
10^6	4	3e-01 (8.1)	0.3 (14.0)	1e-01 (5.7)	0.1 (16.4)	1e+00 (8.2)	0.9 (11.6)
10^6	8	3e-01 (8.5)	0.2 (14.0)	1e-01 (6.5)	0.1 (16.4)	7e-01 (8.7)	0.7 (11.6)
10^6	16	2e-01 (8.9)	0.2 (14.0)	1e-01 (7.1)	0.1 (16.4)	5e-01 (9.0)	0.4 (11.6)
10^6	24	3e-01 (9.0)	0.2 (14.0)	2e-01 (7.4)	0.1 (16.4)	3e-01 (9.0)	0.3 (11.6)
10^6	48	7e-01 (9.2)	0.5 (14.0)	5e-01 (7.8)	0.3 (16.4)	9e-01 (9.3)	0.8 (11.6)
10^7	1	8e+00 (8.2)	3.2 (16.0)	6e+00 (4.0)	2.1 (18.8)	1e+01 (8.8)	5.4 (13.9)
10^7	2	4e+00 (8.6)	1.7 (16.0)	2e+00 (5.4)	0.8 (18.8)	6e+00 (9.0)	3.3 (13.9)
10^7	4	3e+00 (9.0)	1.1 (16.0)	1e+00 (6.0)	0.5 (18.8)	4e+00 (9.1)	2.2 (13.9)
10^7	8	2e+00 (9.2)	0.8 (16.0)	1e+00 (6.8)	0.5 (18.8)	3e+00 (9.8)	1.6 (13.9)
10^7	16	2e+00 (9.6)	0.7 (16.0)	8e-01 (7.5)	0.3 (18.8)	2e+00 (10.0)	1.2 (13.9)
10^7	24	1e+00 (10.0)	0.4 (16.0)	9e-01 (7.8)	0.3 (18.8)	2e+00 (10.0)	1.0 (13.9)
10^7	48	3e+00 (10.0)	1.2 (16.0)	1e+00 (8.4)	0.5 (18.8)	3e+00 (10.6)	1.4 (13.9)
10^8	1	7e+01 (8.8)	4.8 (17.6)	6e+01 (5.1)	3.6 (20.8)	7e+01 (10.0)	6.0 (16.0)
10^8	2	3e+01 (8.9)	2.2 (17.6)	2e+01 (5.3)	1.4 (20.8)	4e+01 (10.0)	3.0 (16.0)
10^8	4	2e+01 (9.3)	1.2 (17.6)	1e+01 (6.1)	0.7 (20.8)	2e+01 (10.5)	1.8 (16.0)
10^8	8	1e+01 (9.9)	0.8 (17.6)	7e+00 (6.7)	0.4 (20.8)	2e+01 (11.0)	1.2 (16.0)
10^8	16	7e+00 (10.0)	0.5 (17.6)	5e+00 (7.7)	0.3 (20.8)	1e+01 (11.0)	0.9 (16.0)
10^8	24	8e+00 (10.1)	0.5 (17.6)	6e+00 (8.0)	0.4 (20.8)	1e+01 (11.3)	0.8 (16.0)
10^8	48	9e+00 (10.9)	0.7 (17.6)	6e+00 (8.6)	0.4 (20.8)	1e+01 (11.9)	0.8 (16.0)
10^9	1	6e+02 (9.3)	4.7 (19.0)	6e+02 (4.7)	3.6 (23.4)	6e+02 (11.0)	5.1 (18.0)
10^9	2	3e+02 (9.7)	2.0 (19.0)	2e+02 (5.5)	1.4 (23.4)	3e+02 (11.0)	2.2 (18.0)
10^9	4	1e+02 (10.0)	1.1 (19.0)	1e+02 (6.5)	0.7 (23.4)	2e+02 (11.7)	1.2 (18.0)
10^9	8	1e+02 (10.1)	0.7 (19.0)	7e+01 (7.0)	0.4 (23.4)	1e+02 (12.0)	0.9 (18.0)
10^9	16	6e+01 (10.9)	0.5 (19.0)	5e+01 (8.0)	0.3 (23.4)	7e+01 (12.0)	0.5 (18.0)
10^9	24	6e+01 (11.0)	0.5 (19.0)	5e+01 (8.2)	0.3 (23.4)	6e+01 (12.4)	0.5 (18.0)
10^9	48	6e+01 (11.0)	0.4 (19.0)	5e+01 (8.8)	0.3 (23.4)	6e+01 (13.0)	0.5 (18.0)

Table 4: Comparison between CPU and GPU versions of Algorithm 4 implemented in `NewtonCQK.jl` using 64 bit floating-point. Times are in milliseconds, and were taken as the median over the 20 generated instances. The values between parentheses are the mean of iterations.

report results for the first and last 100 SPG iterations. For a more comprehensive comparison, we include the Julia implementation of Condat’s method by Dai and Chen; this allows for a more integrated and consistent comparison within our SPG framework, which is developed in the same language. To ensure a fair evaluation, the `NewtonCQK.jl` implementation is configured to return sparse vectors, matching the default output of the Dai and Chen code.

The `NewtonCQK.jl` implementations outperform Dai and Chen’s code in all scenarios, which confirms the results presented in Section 5.2. Indeed, the projection onto the ℓ_1 -ball involves computing a projection onto the simplex as a sub-procedure. Finally, we note that the implementation by Dai and Chen does not support a warm start strategy.

We observe that the warm start is beneficial only for the SC_{11} case but not for SC_1 . In SC_1 , the solution is almost fully dense and the sparsity structure seems to greatly vary, even in the final iterations. In this case, using the previous iterate to guess the initial multiplier is not effective, as the free variable set is not stabilizing. On the other hand, for SC_{11} the solution is sparse and the variation of the free variable set is smaller leading to big gains at the final projections.

The performance of the `NewtonCQK.jl` parallel implementation is shown in Figure 8. As observed in Section 5.1.2, the performance gain from parallelism is consistent throughout the SPG execution, but remains limited to 8 to 16 threads due to the modest problem sizes. Notably, higher speedups are observed for the SC_{11} instance, where the iterates are highly sparse.

6 Conclusions

In this paper, we revisited the semi-smooth Newton method proposed in [14] for solving the continuous quadratic knapsack problem (CQK), a fundamental model that arises in various optimization contexts. We discussed how this Newton method can be efficiently parallelized, with a particular focus on projections onto the simplex and ℓ_1 -ball. Our open-source Julia package, `NewtonCQK.jl`, provides high-performance CPU and GPU implementations that are both flexible and easy to integrate. Extensive numerical experiments demonstrate that our implementation outperforms state-of-the-art algorithms, including the widely adopted variable-fixing method of Condat [15]. Furthermore, we showcased the scalability of our approach for large-scale problems; notably, our GPU implementation achieves speedups of 45–186 times compared to its sequential CPU counterpart for problems with one million variables or more.

Declaration of competing interest

The authors declare that they have no known competing financial interests or personal relationships that could have appeared to influence the work reported in this paper.

Acknowledgments

This work was supported by CEPID-CeMEAI (FAPESP 2013/07375-0), FAPESP (grants 2023/08706-1 and 2024/12967-8) and CNPq (grants 312394/2023-3 and 302520/2025-2). This research used computational resources from CENAPAD-SP (Centro Nacional de Processamento de Alto Desempenho em São Paulo), Unicamp / FINEP - MCTI.

References

- [1] A. R. Amaral. On the exact solution of a facility layout problem. *European Journal of Operational Research*, 173(2):508–518, sep 2006.
- [2] C. Bauer and Et al. OhMyThreads.jl simple multithreading in Julia, 2026. <https://github.com/JuliaFolds2/OhMyThreads.jl>.
- [3] R. Behling, Y. Bello-Cruz, L.-R. Santos, and P. J. S. Silva. Basis pursuit by inconsistent alternating projections. (arXiv:2508.15026), Aug. 2025. arXiv:2508.15026 [math].
- [4] M. Besançon, T. Papamarkou, D. Anthoff, A. Arslan, S. Byrne, D. Lin, and J. Pearson. Distributions.jl: Definition and modeling of probability distributions in the juliastats ecosystem. *Journal of Statistical Software*, 98(16):1–30, 2021.
- [5] E. G. Birgin, J. M. Martínez, and M. Raydan. Nonmonotone spectral projected gradient methods on convex sets. *SIAM Journal on Optimization*, 10(4):1196–1211, 2000.
- [6] E. G. Birgin, J. M. Martínez, and M. Raydan. Algorithm 813: SPG-software for convex-constrained optimization. *ACM Transactions on Mathematical Software*, 27(3):340–349, 2001.

- [7] G. R. Bitran and A. C. Hax. Disaggregation and resource allocation using convex knapsack problems with bounded variables. *Management Science*, 27(4):431–441, Apr. 1981.
- [8] K. M. Bretthauer and B. Shetty. Quadratic resource allocation with generalized upper bounds. *Operations Research Letters*, 20(2):51–57, Feb. 1997.
- [9] K. M. Bretthauer and B. Shetty. The nonlinear knapsack problem – algorithms and applications. *European Journal of Operational Research*, 138(3):459–472, May 2002.
- [10] K. M. Bretthauer, B. Shetty, and S. Syam. A branch and bound algorithm for integer quadratic knapsack problems. *ORSA Journal on Computing*, 7(1):109–116, Feb. 1995.
- [11] C. J. Burges. A tutorial on support vector machines for pattern recognition. *Data Mining and Knowledge Discovery*, 2(2):121–167, 1998.
- [12] J. Chen and J. Revels. Robust benchmarking in noisy environments. *arXiv e-prints*, Aug 2016.
- [13] S. S. Chen, D. L. Donoho, and M. A. Saunders. Atomic decomposition by basis pursuit. *SIAM Review*, 43(1):129–159, 2001.
- [14] R. Cominetti, W. F. Mascarenhas, and P. J. S. Silva. A Newton’s method for the continuous quadratic knapsack problem. *Mathematical Programming Computation*, 6(2):151–169, Feb. 2014.
- [15] L. Condat. Fast projection onto the simplex and the l_1 ball. *Mathematical Programming*, 158(1–2):575–585, Sept. 2016.
- [16] Y. Dai and C. Chen. Sparsity-exploiting distributed projections onto a simplex. *INFORMS Journal on Computing*, 36(3):820–835, May 2024.
- [17] Y.-H. Dai and R. Fletcher. New algorithms for singly linearly constrained quadratic programs subject to lower and upper bounds. *Mathematical Programming*, 106(3):403–421, Oct. 2005.
- [18] J. Dean and S. Ghemawat. Mapreduce: simplified data processing on large clusters. *Communications of the ACM*, 51(1):107–113, Jan. 2008.
- [19] J. Duchi, S. Shalev-Shwartz, Y. Singer, and T. Chandra. Efficient projections onto the l_1 -ball for learning in high dimensions. In *Proceedings of the 25th international conference on Machine learning - ICML '08*, ICML '08, pages 272–279. ACM Press, 2008.
- [20] R. Fletcher, S. Leyffer, D. Ralph, and S. Scholtes. Local convergence of SQP methods for mathematical programs with equilibrium constraints. *SIAM Journal on Optimization*, 17(1):259–286, 2006.
- [21] M. D. Gonzalez-Lima, W. W. Hager, and H. Zhang. An affine-scaling interior-point method for continuous knapsack constraints with application to support vector machines. *SIAM Journal on Optimization*, 21(1):361–390, Jan. 2011.
- [22] K. C. Kiwiel. Breakpoint searching algorithms for the continuous quadratic knapsack problem. *Mathematical Programming*, 112(2):473–491, Nov. 2008.
- [23] K. C. Kiwiel. Variable fixing algorithms for the continuous quadratic knapsack problem. *Journal of Optimization Theory and Applications*, 136(3):445–458, Nov. 2008.
- [24] R. Lopes, S. A. Santos, and P. J. S. Silva. Accelerating block coordinate descent methods with identification strategies. *Computational Optimization and Applications*, 72(3):609–640, Jan. 2019.
- [25] G. Marsaglia. Xorshift RNGs. *Journal of Statistical Software*, 8(14), 2003.
- [26] C. Michelot. A finite algorithm for finding the projection of a point onto the canonical simplex of \mathbb{R}^n . *Journal of Optimization Theory and Applications*, 50(1):195–200, July 1986.

- [27] J. Nocedal and S. J. Wright. *Numerical Optimization*. Springer, 2 edition, 2006.
- [28] J.-S. Pang. A new and efficient algorithm for a class of portfolio selection problems. *Operations Research*, 28(3-part-ii):754–767, 1980.
- [29] M. Patriksson. A survey on the continuous nonlinear resource allocation problem. *European Journal of Operational Research*, 185(1):1–46, Feb. 2008.
- [30] T. C. Sharkey, H. E. Romeijn, and J. Geunes. A class of nonlinear nonseparable continuous knapsack and multiple-choice knapsack problems. *Mathematical Programming*, 126(1):69–96, Jan. 2011.
- [31] R. Tibshirani. Regression shrinkage and selection via the lasso. *Journal of the Royal Statistical Society. Series B (Methodological)*, 58(1):267–288, 1996.
- [32] J. A. Ventura. Computational development of a lagrangian dual approach for quadratic networks. *Networks*, 21(4):469–485, 1991.

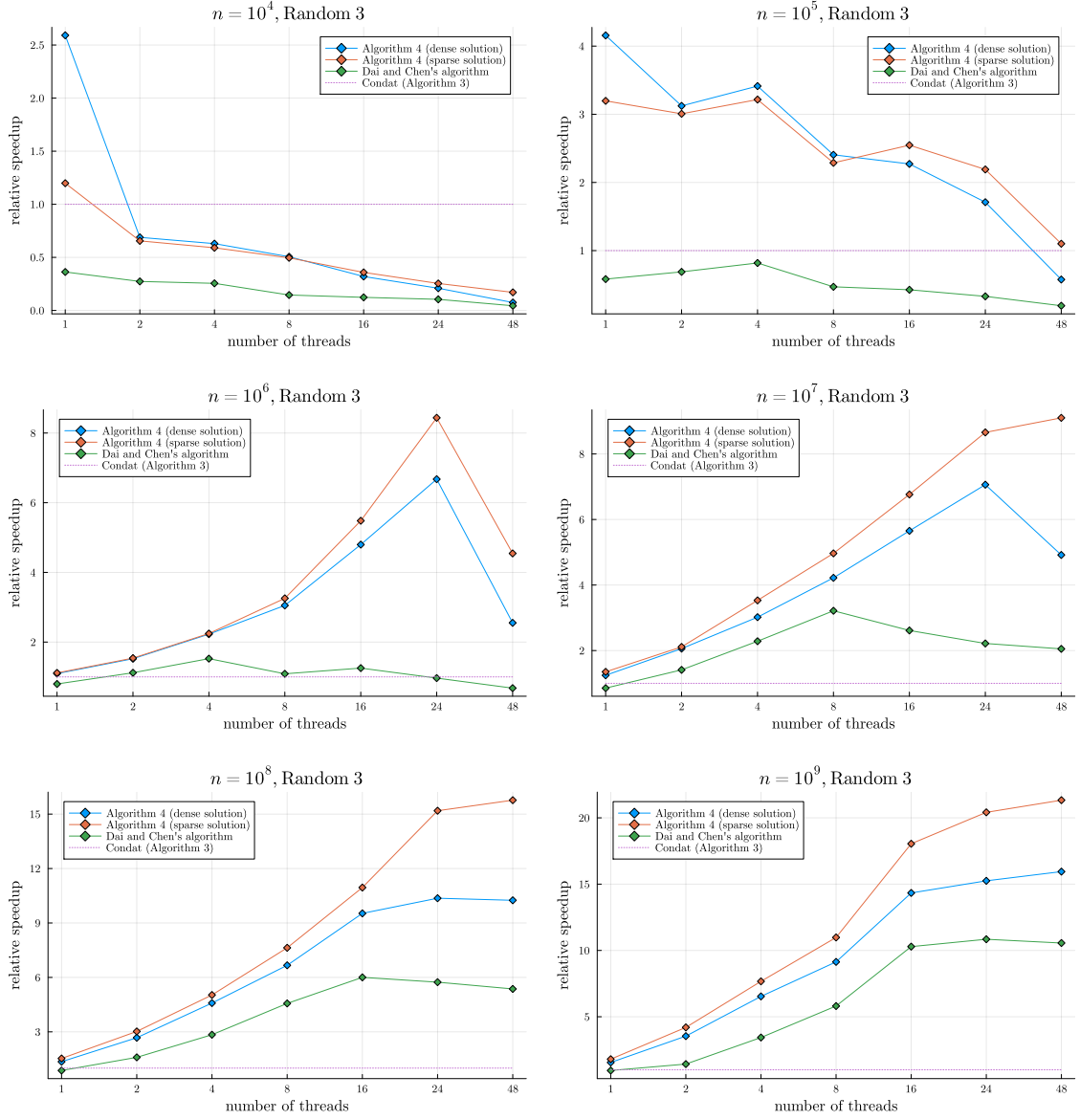


Figure 6: Speedups of Algorithm 4 implemented in `NewtonCQK.jl` (CPU versions returning dense and sparse solutions), Dai and Chen's (sparse solution) and Condat's (dense solution) algorithms on $(\text{proj}\Delta)$, instances of type 3. The base algorithm is of Condat, which is represented by the horizontal line.

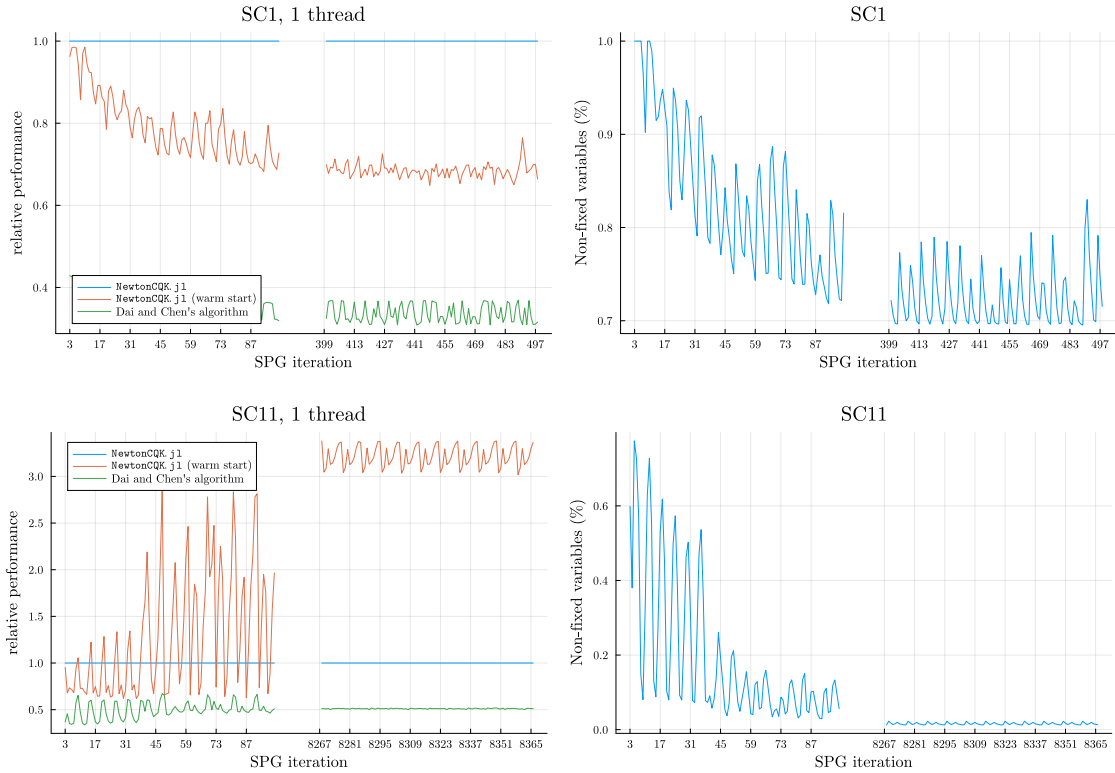


Figure 7: On the left, relative performance of CPU algorithms that compute sparse projections onto the ℓ_1 -ball along the SPG iterations. `NewtonCQK.jl` implementation of the specialized Algorithm 1 with no warm start is the base (horizontal line). On the right, the percentage of non-fixed variables of SPG iterates.

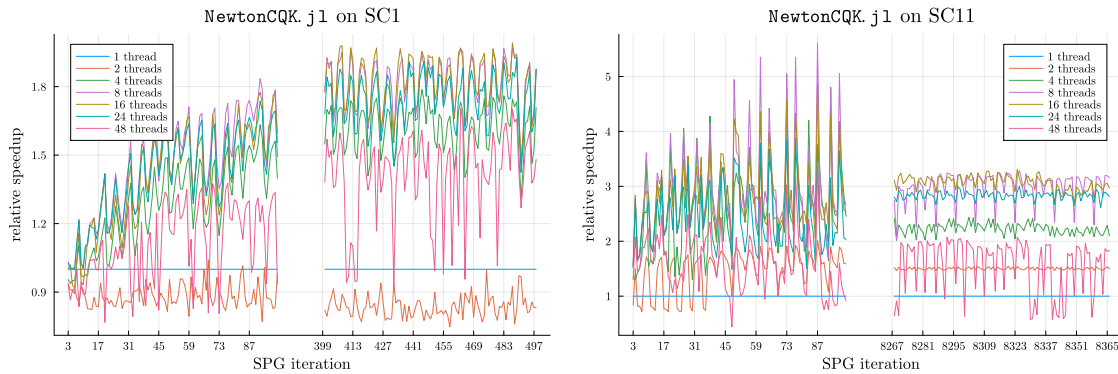


Figure 8: Speedups of the parallel implementation of the specialized Algorithm 1 from `NewtonCQK.jl` for solving (9) (returning sparse solutions) in relation to the sequential variant along the SPG iterations. All algorithms were executed using the current SPG iterate as warm start.